Carbon burning rates on the compound nucleus formation

Masahiko Katsuma[1,2,*]

[1]Advanced Mathematical Institute, Osaka City University, Osaka 558-8585, Japan
[2]Institut d'Astronomie et d'Astrophysique, Université Libre de Bruxelles, B-1050 Brussels, Belgium

Abstract. The ^{12}C+^{12}C reaction rates based on the compound nucleus formation seem to be concordant with the standard rates. The resonant contribution in ^{12}C+^{12}C is also discussed. To put the rates on firm ground, the resonances below $E_{c.m.}$ = 3 MeV will have to be studied further.

1 Introduction

The ^{12}C+^{12}C fusion reaction is one of the key reactions to understand the evolution of massive stars and various explosive scenarios. However, precise measurements of cross sections below $E_{c.m.}$ = 3 MeV are difficult because of the tiny amplitudes caused by the Coulomb barrier. At present, the direct measurements have been performed in $E_{c.m.}$ = 2.1–2.5 MeV [1]. The indirect measurements have been studied with ^{24}Mg(α,α') [2] and Trojan horse method [3]. The derived rates [3] are much faster than CF88 [4], due to the resonant states at $E_{c.m.} \approx 1.5$ MeV, which may have the ^{12}C+^{12}C molecule-like structure. The nuclear fusion for ^{12,13}C+^{13}C have also been discussed experimentally to understand C+C comprehensively [5].

In this presentation, I use a barrier penetration model (BPM), and I show the calculated results of isotope dependence of fusion cross sections and reaction rates in C+C. The transmission coefficients are given by the WKB approximation, semi-classically, and the potentials used in the present work are calculated from a single-folding model [6] with [7, 8]. I also discuss the contribution from the resonances in ^{12}C+^{12}C by comparing the result of BPM with a schematic calculation of the coupled-channels multi-level *R*-matrix [9].

2 Compound nucleus formation

Before moving on to the results, let me recall the compound nucleus (CN) formation, to understand the reaction mechanism in C+C. The ^{12}C+^{12}C potential obtained from the studies of elastic scattering has predicted the sequences of the rotational excitation in ^{24}Mg [7, 10]. These resonances are the excited states with the ^{12}C+^{12}C molecule-like structure in ^{24}Mg. However, the potential resonances at $E_{c.m.} \approx 0$ are dispersed easily, because of the couplings to reaction channels. Although the inelastic channels are closed at $E_{c.m.}$ = 4.44 MeV, other reaction channels are open, and they work as absorption to the entrance channel. Accordingly, their fragments are distributed around the original energy positions. In fact, many fragments of $J^\pi = 2^+, 4^+$ resonances have been observed, in addition to 0^+ [3]. Whereas most of flux are consumed by Coulomb scattering, a small amount of flux is captured into the long-living fragment levels, and exits through the proton, neutron, and α channels after forming a compound nucleus. Under the circumstance, the reactions should be described statistically,

*e-mail: mkatsuma@gmail.com

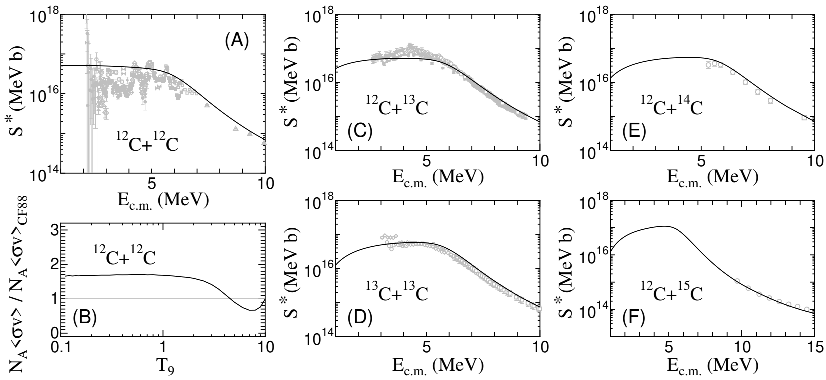

Figure 1. Comparison in S^* between BPM and experimental data: (A) ^{12}C+^{12}C, (C) ^{12}C+^{13}C, (D) ^{13}C+^{13}C, (E) ^{12}C+^{14}C, and (F) ^{12}C+^{15}C. The solid curves are the results with BPM. The experimental data are taken from [1, 5, 11, 12]. (B) The derived rates of ^{12}C+^{12}C are shown in ratio of CF88 [4].

and the emitted nuclei have to be treated as evaporation products. Therefore, I adopt BPM and *R*-matrix based on the CN formation in the present study.

In BPM, the energy-averaged fusion cross sections are given by $\sigma_F = (\pi/k^2)\sum_L(2L+1)\langle|S_{CN}|^2\rangle$. k is the wavenumber; L is the angular momentum between nuclei. $\langle|S_{CN}|^2\rangle$ are the transmission coefficients T_L, given by WKB approximation for $E_{c.m.} < E_B$: $T_L = \{1 + \exp[2\int_{R_1}^{R_2} K(R)\,dR]\}^{-1}$, $K(R) = \{(2\mu)/\hbar^2[\tilde{U}_L(R) - E_{c.m.}]\}^{1/2}$. E_B is the barrier height energy. μ is the reduced mass. R_1 and R_2 are the inner and outer turning points of effective potentials $\tilde{U}_L$. The nuclear potentials in $\tilde{U}_L$ are calculated recursively from the single-folding model [6–8]. The cross sections are also given by *R*-matrix theory, $\sigma_F = (\pi/k^2)\sum_{cL}(2L+1)\,|S^L_{c,0}|^2$. $S^L_{c,0}$ is the S-matrix deduced from the *R*-matrix with the resonance parameters in [3]. The reduced width of ^{12}C+^{12}C is statistically assumed to be a constant $\gamma^2_{iL} = 0.001\gamma^2_W$ for all levels, based on the CN formation. γ^2_W is the Wigner limit. In [5], the transmission coefficients are calculated from an approximation using the unitarity relation of S-matrix. To display the cross sections, the S^* factors are defined as $S^* \equiv \sigma_F E_{c.m.} \exp(87.21E_{c.m}^{-1/2}+0.46E_{c.m.})$, e.g. [3].

3 Results & Conclusion

The calculated S^* factors with BPM for ^{12}C+^{12}C are shown by the solid curve in Fig. 1(A), and they appear to give the trend of the energy variation in the experimental data [1, 11]. The derived reaction rates are shown in ratio to CF88. (Fig. 1(B)) They seem consistent with CF88. For ^{12,13}C+^{13}C and ^{12}C+^{14,15}C, the present calculations of BPM (solid curves) reproduce the experimental data [5, 12], consistently, as shown in Figs. 1(C) – 1(F).

Figure 2(A) illustrates the isotope dependence of S^* obtained from BPM. In BPM, the ^{12}C+^{12}C S^* factors below $E_{c.m.} = 2$ MeV become the largest, so the derived reaction rates are the fastest below $T_9 = 0.8$ (Fig. 2(B)). In addition, the S^* factors are found to be enhanced at the sub-barrier energies as the number of neutrons increases. Particularly, those of ^{12}C+^{15}C are enhanced larger. The barrier radius R_B and barrier height energy E_B in the present calculations are shown in Figs. 2(C) and 2(D), as a function of the mass number. R_B (E_B) becomes large (small) as the number of neutrons increases. Especially, R_B suddenly becomes large at ^{15}C. This is caused by the weakly-bound s-wave neutron in ^{15}C. Therefore, the corresponding S^* and reaction rates are expected to be enhanced more by the sharp reduction of E_B.

The resonant contribution in ^{12}C+^{12}C is shown in Fig. 3. From the result of the *R*-matrix calculation by the solid curve in Fig. 3(A), the values of S^* are found to be much smaller than those of [3]. In the present calculation, I include the same 34 levels and four exit channels as

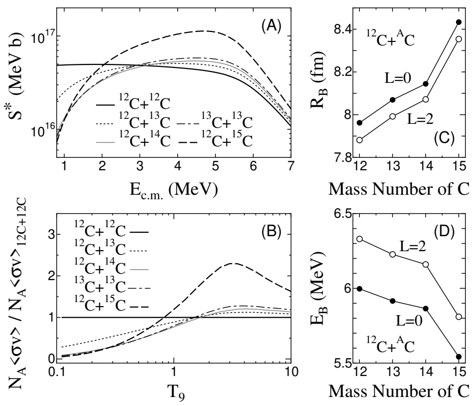

Figure 2. Isotope dependence of (A) S^*, (B) reaction rates, (C) R_B, and (D) E_B, obtained from BPM. (A,B) The curves are the results for the respective system shown in figure. (C,D) R_B and E_B are obtained from $\tilde{U}_L$. The solid and open circles are the values for $L = 0$ and $L = 2$, respectively.

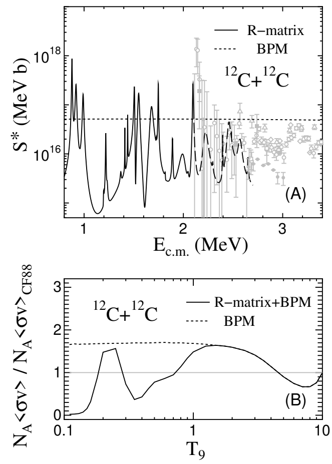

Figure 3. (A) Low-energy extrapolation of S^* and (B) the reaction rates. The solid and dotted curves are the results calculated from *R*-matrix and BPM. The experimental data are taken from [1, 11].

those in [3]. If $\gamma_{iL}^2 = 0.05\gamma_W^2$ is used as the reduced width of ^{12}C+^{12}C at $E_{c.m.} \approx 1.5$ MeV, the reaction rates would increase like those in [3]. The carbon burning rates are sensitive to the reduced width of ^{12}C+^{12}C. In addition, the reaction rates estimated from the *R*-matrix extrapolation are confirmed to be reduced from the result of BPM. However, the derived rates at $T_9 = 0.6$ still seem to be consistent with CF88. To put the rates on firm ground, the resonances below $E_{c.m.} = 3$ MeV will have to be scrutinized further.

Acknowledgements

I thank Prof. X.D. Tang for his valuable comments and providing me with the experimental data.

References

[1] W.P. Tan *et al.*, PRL **124**, 192702 (2020); G. Fruet *et al.*, PRL **124**, 192701 (2020); C.L. Jiang *et al.*, PRC **97**, 012801(R) (2018); T. Spillane *et al.*, PRL **98**, 122501 (2007)
[2] T. Kawabata *et al.*, J. Phys. Conf. **436**, 012009 (2013)
[3] A. Tumino *et al.*, Nature **557**, 687 (2018); Springer Proc. Phys. **219**, 17 (2019)
[4] G.R. Caughlan, W.A. Fowler, Atom. Data Nucl. Data Tables **40**, 283 (1988)
[5] M. Notani *et al.*, PRC **85**, 014607 (2012); X.D. Tang, Springer Proc. Phys. **219**, 13 (2019); B.B. Back *et al.*, Rev. Mod. Phys. **86**, 317 (2014)
[6] H. Nishioka *et al.*, Nucl. Phys. A **415**, 230 (1984)
[7] Y. Kondō, M. Katsuma, Nucl. Phys. A **738**, 226 (2004); Y. Kondō, M.E. Brandan, G.R. Satchler, Nucl. Phys. A **637**, 175 (1998)
[8] B.A. Watson *et al.*, Phys. Rev. **182**, 977 (1969)
[9] A.M. Lane, R.G. Thomas, Rev. Mod. Phys. **30**, 257 (1958)
[10] M.E. Brandan, G.R. Satchler, Phys. Rep. **285**, 143 (1997)
[11] E.F. Aguilera *et al.*, PRC **73**, 064601 (2006); D.G. Kovar *et al.*, PRC **20**, 1305 (1979); B. Dasmahapatra *et al.*, Nucl. Phys. A **384**, 257 (1982); M.D. High, B. Čujec, Nucl. Phys. A **282**, 181 (1977); H.W. Becker *et al.*, Z. Phys. A **303**, 305 (1981)
[12] EXFOR, International Network of Nuclear Reaction Data Centres (NNDC); Nuclear Reaction Video (NRV) project supported by Russian Foundation for Basic Research